Explicit Finite Element Artificial Boundary Scheme for Seismic Soil-Structure Interaction Analysis

Mi Zhao & Xiuli Du
The Key Laboratory of Urban Security and Disaster Engineering of Ministry of Education, Beijing University of Technology, Beijing 100124, China

Jingbo Liu
Department of Civil Engineering, Tsinghua University, Beijing 100084, China

SUMMARY:
A time-domain direct method is used to solve the seismic soil-structure interaction problem, which combines the explicit finite element method and a high-order accurate artificial boundary condition. A seismic wave input method is presented as follows. From the given input wave as the displacement motion of rigid rock, the free field displacements at artificial boundary nodes are first obtained in time domain by analyzing a one-dimensional soil column model using the finite element method. The equivalent forces on artificial boundary nodes are then derived by resisting both the near-field finite element model and the artificial boundary condition to maintain the nodal free field displacements. The effectiveness of the method combining the time-domain direct method with the seismic wave input method is demonstrated by analyzing an underground structure in an unbounded soil layer resting on a rigid rock under the out-of-plane shear seismic waves.

Keywords: Soil-structure interaction; Finite element method; Artificial boundary condition; Seismic wave input

1. INTRODUCTION

Seismic soil-structure interaction (Wolf 1988) is a wave propagation problem on unbounded media, where the nonlinearity of structure and its adjacent soil usually requires considering. To numerically solve this problem in time domain, the finite element method can be used to simulate the near field that is a finite domain obtained by introducing a so-called artificial boundary to enclose the structure and its adjacent soil. A time-domain artificial boundary condition (ABC) requires enforcing on the artificial boundary of near field to model the radiation damping effect of the truncated far field that is a residual infinite domain with regularity in material and geometry properties. Seismic waves arising from far field should be inputted as a kind of excitation on the artificial boundary of near field.

The state-of-arts about ABCs can see Zhao et al. (2011) and references therein. A general methodology has been presented in Zhao et al. (2010, 2011) for developing the high-order accurate ABC and resulting in the explicit finite element artificial boundary scheme. The methodology can be stated as follows. First, an exact ABC of force-displacement type (also called Dirichlet-to-Neumann (DtN) type (Givoli 1999)) is constructed by solving the initial boundary value problem of far field using a fully analytical method. It is global in time due to the presence of temporal convolution, leading to the unacceptable high costs for the large-scale problem and long-time computation. Second, a method to localize temporal convolution is then proposed to increase computational efficiency, which combines the frequency-domain rational function approximation based on a stable identification method (Du and Zhao 2010a) and the time-domain auxiliary variable realization as a second-order ordinary differential equation system or as a new lumped-parameter mechanical model with physical meaning (Du and Zhao 2010b). In theory, the whole approximate process makes the accuracy of ABC not lower than that of finite element method, as its order number increase to a moderate large value. Third, the resulting temporally local ABC is incorporated into the near-field finite element model. The coupled equation system is formed and solved by a new explicit time integration algorithm (Wang et al. 2008). To the best of authors' knowledge, this is so far only a fully explicit solution process for the near- and far-field systems by using a single time integration algorithm. Two types of problems of the

transient scalar wave propagation in two-dimensional unbounded media, i.e., the waveguide problem and the exterior problem, have been considered in Zhao et al. (2011) and Zhao et al. (2010), respectively. Both of them are defined according to the material and geometry properties of far field. The former corresponds to an unbounded soil layer on rigid rock, and the latter to an unbounded half space with circular cavity.

Seismic wave input method should match with the time-domain direct method combining the artificial boundary condition with the finite element method. For the well-known viscous boundary (Lysmer and Kuhlemeyer 1969), Joyner and Chen (1975) successfully solved the wave motion input for one-dimensional model by means of converting incident motion into an equivalent load acted on the artificial boundary. Yasui et al. (1988) presented an amended method based on Joyner and Chen (1975), that can treat approximately slant body wave input in finite element method. The third author and his co-worker (Liu and Lü 1997) proposed the so-called viscous-spring boundary and the corresponding seismic wave input method. Note that both the viscous and viscous-spring boundaries have the form of force-displacement relation on artificial boundary just as the above high-order accurate ABC. Therefore, the ideas in above seismic wave input methods can be applicable to the time-domain direct method proposed by authors.

In this paper, a time-domain direct method is presented to analyzing the seismic soil-structure interaction problem. The explicit finite element artificial boundary scheme in Zhao et al. (2011) is used, where the high-order accurate ABC is reformulated based on the semi-analytical method (Zienkiewicz and Taylor 2008). Some semi-analytical ABCs and their improvements (Lysmer and Waas 1972, Guddati and Tassoulas 1999, Liu and Xu 2002, Liu and Zhao 2010, Birk and Ruge 2007, Bazyar and Song 2008) have arisen. A seismic wave input method that is suitable for the high-order accurate ABC is presented based on the idea in Liu and Lü (1997). Using the time-domain direct method, we analyzed a simple example of an underground structure in an unbounded soil layer on rigid rock subjected to the out-of-plane shear seismic waves.

2. PROBLEM STATEMENT

This paper considers a general structure in an unbounded soil layer resting on a rigid rock subjected to the out-of-plane shear seismic waves. This seismic soil-structure interaction problem is shown in Fig. 2.1. The Cartesian coordinate system (x,y) is chosen. The given seismic wave motion is the out-of-plane displacement $u_0(t)$ of rigid rock, where t denotes time. Two vertical artificial boundaries are introduced to divide the whole unbounded media into the near and far fields. The near field involves all nonlinearity and irregularity, and the far field is a homogenous linear isotropic soil layer of semi-infinite length and constant depth b.

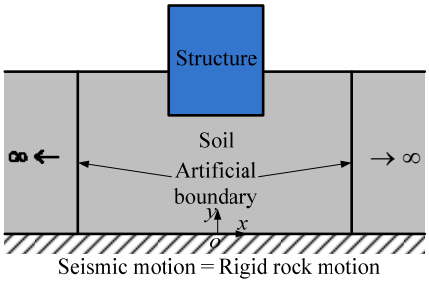

Figure 2.1. Seismic soil-structure interaction problem

The near field is modeled by the finite element method. For simplicity, we assume the linear near field and consider only one artificial boundary in the following derivation. The finite element equation of near field can be written as the following matrix form partitioned according to the artificial boundary nodes (subscript B) and the remaining interior finite element nodes (subscript I)

$$\begin{bmatrix} \mathbf{M}_{\mathrm{I}} & \mathbf{0} \\ \mathbf{0} & \mathbf{M}_{\mathrm{B}} \end{bmatrix} \begin{Bmatrix} \ddot{\mathbf{u}}_{\mathrm{I}} \\ \ddot{\mathbf{u}}_{\mathrm{B}} \end{Bmatrix} + \begin{bmatrix} \mathbf{C}_{\mathrm{I}} & \mathbf{C}_{\mathrm{IB}} \\ \mathbf{C}_{\mathrm{BI}} & \mathbf{C}_{\mathrm{B}} \end{bmatrix} \begin{Bmatrix} \dot{\mathbf{u}}_{\mathrm{I}} \\ \dot{\mathbf{u}}_{\mathrm{B}} \end{Bmatrix} + \begin{bmatrix} \mathbf{K}_{\mathrm{I}} & \mathbf{K}_{\mathrm{IB}} \\ \mathbf{K}_{\mathrm{BI}} & \mathbf{K}_{\mathrm{B}} \end{bmatrix} \begin{Bmatrix} \mathbf{u}_{\mathrm{I}} \\ \mathbf{u}_{\mathrm{B}} \end{Bmatrix} = \begin{Bmatrix} \mathbf{0} \\ \mathbf{f}_{\mathrm{B}} \end{Bmatrix} \tag{2.1}$$

where **M** is the mass matrix; **C** is the damping matrix; **K** is the stiffness matrix; **u**=**u**(*t*) is the nodal displacement vector, which is the total and absolute displacements; the dot over variable denotes a derivative to time *t*; **0** denotes no load acting on near field is considered; and $\mathbf{f}_{\mathrm{B}}=\mathbf{f}_{\mathrm{B}}(t)$ is the action force vector of far field to near field. The interior finite element nodes include the rigid rock nodes, which satisfy the forced displacement boundary condition and have the same displacement $u_0(t)$.

The far field is truncated. Its action to near field is considered by imposing $\mathbf{f}_{\mathrm{B}}$ on artificial boundary. According to the assumption of material and geometry of far field, the responses in far field satisfy the principle of superposition. With respect to the radiation damping effect and the seismic wave input, respectively, we decompose the total responses in far field (including artificial boundary) into the scattering wave field response (without the incoming wave from far field into near field and the wave propagating parallel to artificial boundary) and the free wave field response (without the outgoing wave from near field into far field). Concretely, the displacements and forces on artificial boundary nodes can be decomposed as

$$\mathbf{u}_{\mathrm{B}} = \mathbf{u}_{\mathrm{Bs}} + \mathbf{u}_{\mathrm{Bf}} \tag{2.2}$$

$$\mathbf{f}_{\mathrm{B}} = \mathbf{f}_{\mathrm{Bs}} + \mathbf{f}_{\mathrm{Bf}} \tag{2.3}$$

where the subscripts s and f denote the scattering-field and free-field responses, respectively. The scattering-field response is modeled by the artificial boundary condition, and the free-field response is applied by the seismic wave input method.

3. ARTIFICIAL BOUNDARY CONDITION

The artificial boundary condition is a relation between the force $\mathbf{f}_{\mathrm{Bs}}(t)$ and displacement $\mathbf{u}_{\mathrm{Bs}}(t)$ (and its derivative to time) of scattering wave field on artificial boundary nodes. It is obtained from the initial boundary value problem of far field. The scattering-field displacement $u_{\mathrm{s}}(x,y,t)$ in far field satisfies the out-of-plane wave equation

$$\frac{\partial^2 u_{\mathrm{s}}}{\partial x^2} + \frac{\partial^2 u_{\mathrm{s}}}{\partial y^2} = \frac{1}{c^2}\frac{\partial^2 u_{\mathrm{s}}}{\partial t^2} \tag{3.1}$$

where $c=\sqrt{G/\rho}$ is the shear wave velocity with shear modulus G and mass density ρ. For the scattering wave field, the fixed boundary condition is satisfied on rigid rock, and the free boundary condition on soil surface. The continuity condition is on artificial boundary and the radiation condition at infinity. The far field is at rest initially.

Eqn. (3.1) is discretized along only the *y* coordinate using the standard Galerkin finite element process. The scattering-field displacement is approximated as

$$u_{\mathrm{s}} \approx \mathbf{N}\mathbf{u}_{\mathrm{s}} \tag{3.2}$$

where $\mathbf{u}_{\mathrm{s}}=\mathbf{u}_{\mathrm{s}}(x,t)$ is the column vector of the displacements on the discrete lines of constant *y* coordinate; and $\mathbf{N}=\mathbf{N}(y)$ is the row vector of the global shape functions that can be chosen simply as the linear one-dimensional shape functions. The semi-discrete form of Eqn. (3.1) can thus be written as

$$\mathbf{W}_1 \frac{\partial^2 \mathbf{u}_s}{\partial x^2} - \mathbf{W}_2 \mathbf{u}_s = \frac{1}{c^2} \mathbf{W}_1 \frac{\partial^2 \mathbf{u}_s}{\partial t^2} \tag{3.3}$$

with the symmetric positive define matrices

$$\mathbf{W}_1 = \int_0^b \mathbf{N}^{\mathrm{T}} \mathbf{N} \mathrm{d}y \tag{3.4}$$

$$\mathbf{W}_2 = \int_0^b \frac{\partial \mathbf{N}^{\mathrm{T}}}{\partial y} \frac{\partial \mathbf{N}}{\partial y} \mathrm{d}y \tag{3.5}$$

where the superscript T denotes transposition. The spatially two-dimensional problem is thus reduced to the one-dimensional one.

Eqn. (3.3) is diagonalized by eigenvalue decomposition of coefficient matrices. The generalized eigenvalue problem with respect to $\mathbf{W}_1$ and $\mathbf{W}_2$ is

$$\mathbf{W}_2 \boldsymbol{\varphi} = \lambda^2 \mathbf{W}_1 \boldsymbol{\varphi} \tag{3.6}$$

where λ and $\boldsymbol{\varphi}$ are eigenvalue and eigenvector, respectively. Due to the symmetric positive definition of $\mathbf{W}_1$ and $\mathbf{W}_2$, all eigenvalues are positive real and all eigenvectors are orthogonal. If the first L eigenmodes are considered, $\mathbf{u}_s$ can be expanded with respect to the modal variable $\hat{\mathbf{u}}_s = \hat{\mathbf{u}}_s(x,t)$ as

$$\mathbf{u}_s = \Phi \hat{\mathbf{u}}_s \tag{3.7}$$

with the eigenvector matrix

$$\Phi = \begin{bmatrix} \boldsymbol{\varphi}_1 & \boldsymbol{\varphi}_2 & \cdots & \boldsymbol{\varphi}_L \end{bmatrix} \tag{3.8}$$

Substituting Eqn. (3.7) into Eqn. (3.3) and premultiplying the result by $\boldsymbol{\Phi}^{\mathrm{T}}$ lead to the diagonalized equation

$$\frac{\partial^2 \hat{\mathbf{u}}_s}{\partial x^2} - \Lambda \hat{\mathbf{u}}_s = \frac{1}{c^2} \frac{\partial^2 \hat{\mathbf{u}}_s}{\partial t^2} \tag{3.9}$$

with the diagonal eigenvalue matrix

$$\boldsymbol{\Lambda} = \begin{bmatrix} \lambda_1^2 & & & \\ & \lambda_2^2 & & \\ & & \ddots & \\ & & & \lambda_L^2 \end{bmatrix} \tag{3.10}$$

After the finite element discretization in partial space dimension and the eigenvalue diagonalization, Eqn. (3.1) is transformed into a set of decoupled one-dimensional Eqn. (3.9) that has the same form as Eqn. (7) in Zhao et al. (2011). Starting from Eqn. (3.9) and applying the similar derivation in Zhao et al. (2011), the artificial boundary condition is obtained as a force-displacement relation on artificial boundary

$$\mathbf{f}_{\mathrm{Bs}} = -\left[\mathbf{C}_{\mathrm{B}}^{\infty}\dot{\mathbf{u}}_{\mathrm{Bs}} + \mathbf{K}_{\mathrm{B}}^{\infty}\mathbf{u}_{\mathrm{Bs}} + \sum_{j=1}^{L}\left(\mathbf{C}_{\mathrm{B}j}^{\infty}\dot{\mathbf{u}}_{j}\right)\right] \tag{3.11}$$

with

$$\mathbf{C}_{\mathrm{B}}^{\infty} = \mathbf{W}_1\sum_{j=1}^{L}\left[\left(C_{j,0}+C_{j,1}\right)\boldsymbol{\varphi}_j\boldsymbol{\varphi}_j^{\mathrm{T}}\right]\mathbf{W}_1 \tag{3.12}$$

$$\mathbf{K}_{\mathrm{B}}^{\infty} = \mathbf{W}_1\sum_{j=1}^{L}\left(K_{j,0}\boldsymbol{\varphi}_j\boldsymbol{\varphi}_j^{\mathrm{T}}\right)\mathbf{W}_1 \tag{3.13}$$

$$\mathbf{C}_{\mathrm{B}j}^{\infty} = -\mathbf{W}_1 C_{j,1}\boldsymbol{\varphi}_j\begin{Bmatrix}1 & 0 & \cdots & 0\end{Bmatrix} \tag{3.14}$$

The auxiliary variables $\mathbf{u}_j = \mathbf{u}_j(t)$ $(j=1,\cdots,L)$ satisfy

$$\mathbf{M}_j^{\infty}\ddot{\mathbf{u}}_j + \mathbf{C}_j^{\infty}\dot{\mathbf{u}}_j + \mathbf{C}_{\mathrm{B}j}^{\infty\mathrm{T}}\dot{\mathbf{u}}_{\mathrm{Bs}} = \mathbf{0} \tag{3.15}$$

with

$$\mathbf{M}_j^{\infty} = \begin{bmatrix} M_{j,1} & 0 & 0 & \cdots & 0 & 0 \\ 0 & M_{j,2} & 0 & \cdots & 0 & 0 \\ 0 & 0 & M_{j,3} & \cdots & 0 & 0 \\ \vdots & \vdots & \vdots & \ddots & \vdots & \vdots \\ 0 & 0 & 0 & \cdots & M_{j,N-1} & 0 \\ 0 & 0 & 0 & \cdots & 0 & M_{j,N} \end{bmatrix} \tag{3.16}$$

$$\mathbf{C}_j^{\infty} = \begin{bmatrix} C_{j,1}+C_{j,2} & -C_{j,2} & 0 & \cdots & 0 & 0 \\ -C_{j,2} & C_{j,2}+C_{j,3} & -C_{j,3} & \cdots & 0 & 0 \\ 0 & -C_{j,3} & C_{j,3}+C_{j,4} & \cdots & 0 & 0 \\ \vdots & \vdots & \vdots & \ddots & \vdots & \vdots \\ 0 & 0 & 0 & \cdots & C_{j,L_3-1}+C_{j,N} & -C_{j,N} \\ 0 & 0 & 0 & \cdots & -C_{j,N} & C_{j,N} \end{bmatrix} \tag{3.17}$$

where N is the order number in temporal localization method. In Eqns. (3.12)-(3.14), (3.16) and (3.17), the constants are

$$K_{j,0} = G\lambda_j k_0 \tag{3.18}$$

$$C_{j,l} = \rho c c_l\,, \qquad l=0,\cdots,N \tag{3.19}$$

$$M_{j,l} = \frac{\rho}{\lambda_j}m_l\,, \qquad l=1,\cdots,N \tag{3.20}$$

where the dimensionless constants k_0, c_l and m_l see Table IV for N=5 and Table V for N=21 in Zhao et al. (2011).

For simplicity of denotation, we write the artificial boundary condition Eqns. (3.11) and (3.15) as a mapping relation

$$\mathbf{f}_{\mathrm{Bs}} = -F\left(\mathbf{u}_{\mathrm{Bs}}, \dot{\mathbf{u}}_{\mathrm{Bs}}\right) \tag{3.21}$$

Substituting Eqn. (2.2) and its temporal derivative into Eqn. (3.21), then substituting the result into Eqn. (2.3), and substituting the final result into Eqn. (2.1), lead to

$$\begin{bmatrix} \mathbf{M}_{\mathrm{I}} & \mathbf{0} \\ \mathbf{0} & \mathbf{M}_{\mathrm{B}} \end{bmatrix} \begin{Bmatrix} \ddot{\mathbf{u}}_{\mathrm{I}} \\ \ddot{\mathbf{u}}_{\mathrm{B}} \end{Bmatrix} + \begin{bmatrix} \mathbf{C}_{\mathrm{I}} & \mathbf{C}_{\mathrm{IB}} \\ \mathbf{C}_{\mathrm{BI}} & \mathbf{C}_{\mathrm{B}} \end{bmatrix} \begin{Bmatrix} \dot{\mathbf{u}}_{\mathrm{I}} \\ \dot{\mathbf{u}}_{\mathrm{B}} \end{Bmatrix} + \begin{bmatrix} \mathbf{K}_{\mathrm{I}} & \mathbf{K}_{\mathrm{IB}} \\ \mathbf{K}_{\mathrm{BI}} & \mathbf{K}_{\mathrm{B}} \end{bmatrix} \begin{Bmatrix} \mathbf{u}_{\mathrm{I}} \\ \mathbf{u}_{\mathrm{B}} \end{Bmatrix} + \begin{Bmatrix} \mathbf{0} \\ F\left(\mathbf{u}_{\mathrm{B}}, \dot{\mathbf{u}}_{\mathrm{B}}\right) \end{Bmatrix} = \begin{Bmatrix} \mathbf{0} \\ F\left(\mathbf{u}_{\mathrm{Bf}}, \dot{\mathbf{u}}_{\mathrm{Bf}}\right) + \mathbf{f}_{\mathrm{Bf}} \end{Bmatrix} \tag{3.22}$$

The forth term on the left-hand side of Eqn. (3.22) can combine with the first three terms to form a coupled formulation similar to the left-hand side of Eqn. (73) in Zhao et al. (2011). The right-hand side of Eqn. (3.22) is the load arising from seismic free field. It includes two parts, i.e., the term resisting the artificial boundary condition and the term resisting the near-field finite element model. They are computed in the next section. Eqn. (3.22) can be solved by the standard time integration algorithms in structural dynamics, such as implicit Newmark family. It can also be solved by an explicit algorithm (Wang et al. 2008) if the near-field finite element model has a lumped mass matrix.

4. SEISMIC WAVE INPUT METHOD

From the given seismic wave motion, i.e., the rigid rock displacement $u_0(t)$, the free-field displacement $\mathbf{u}_{\mathrm{Bf}}(t)$ and its temporal derivative are obtained by solving a one-dimensional soil column model using finite element method. The finite element equation of soil column is

$$\mathbf{M}\ddot{\mathbf{u}}_{\mathrm{Bf}} + \mathbf{K}\mathbf{u}_{\mathrm{Bf}} = \mathbf{0} \tag{4.1}$$

with

$$\mathbf{M} = \rho \mathbf{W}_1 \tag{4.2}$$

$$\mathbf{K} = G\mathbf{W}_2 \tag{4.3}$$

where the rigid rock displacement $u_0(t)$ is forced at the bottom of soil column. Eqn. (4.1) can be solved by the standard time integration algorithms in structural dynamics.

The force $\mathbf{f}_{\mathrm{Bf}}(t)$ can be computed from the displacement $\mathbf{u}_{\mathrm{Bf}}(t)$. The free-field displacement on artificial boundary can be approximated as

$$u_{\mathrm{Bf}} \approx \mathbf{N}\mathbf{u}_{\mathrm{Bf}} \tag{4.4}$$

The force is obtained from the surface traction τ_{Bf} on artificial boundary as

$$\mathbf{f}_{\mathrm{Bf}} = \int_0^b \mathbf{N}^{\mathrm{T}} \tau_{\mathrm{Bf}} \mathrm{d}y \tag{4.5}$$

According to the constitutive law

$$\tau = G\frac{\partial u}{\partial x} \tag{4.6}$$

we have

$$\mathbf{f}_{\mathrm{Bf}} = G\mathbf{W}_1\frac{\partial \mathbf{u}_{\mathrm{Bf}}}{\partial x} \tag{4.7}$$

Because the free-field responses do not vary along *x* coordinate, Eqn. (4.7) is equal to zero. This also indicates the fact that in the out-of-plane wave problem the free boundary condition is a symmetric boundary condition. The force will not be zero in the case of two- and three-dimensional elastic wave problems.

5. NUMERICAL EXAMPLES

The dynamic responses of free field site and underground structure, as shown in Fig. 5.1, are analyzed. The out-of-plane seismic wave as Loma Prieta wave shown in Fig. 5.2 is acted on rigid rock.

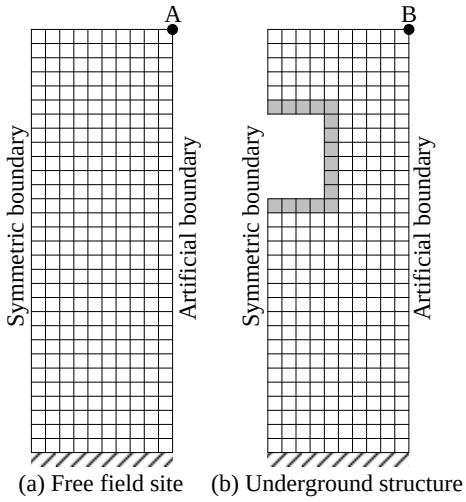

Figure 5.1. Finite element models of free field site and underground structure

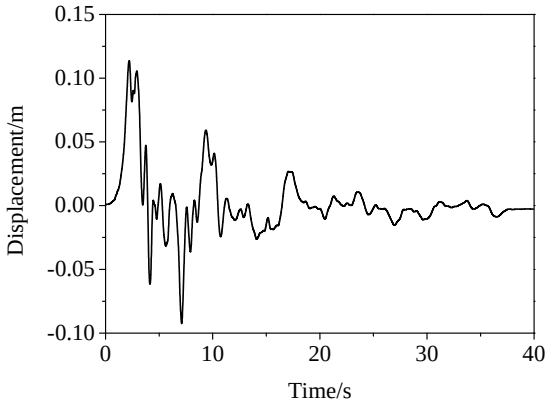

Figure 5.2. Loma Prieta seismic wave

The seismic responses of free field site are first considered. The soil layer resting on rigid rock has height of 30m. The mass density and shear modulus of soil are 2000 kg/m^3 and 80 MPa, respectively, leading to the shear wave velocity 200 m/s. The size of finite element is 1 m×1 m, and the time step is

0.00125 s. Two artificial boundaries are introduced to form the near field of width 20 m. The parameters in the proposed ABC are L=N=5. The displacements at nodes on the same horizontal height are same, and equal to the displacement of one-dimensional soil column at this height. This indicates that the obtained free-field solution is reliable. Because the time history solution is not easy to observe, we give the peak value displacements on artificial boundary nodes. At the instant (7.5675 s) when the relative displacement between point A and rigid rock reaches a peak value (0.2944 m), the relative displacements on artificial boundary nodes are shown in Fig. 5.3. The one-dimensional free field solution is also given as an "exact" reference solution. Clearly, the computational solution using the proposed method is so accurate that it cannot be almost distinguished from the reference solution. The well-known viscous boundary condition (Lysmer and Kuhlemeyer 1969) is also used to solve this problem, where the same seismic wave input method is used. Its solution has the same accuracy as the computational solution using the proposed ABC. This indicates that the free field solution is independent of the type of ABCs due to in this problem no scattering waves that require simulating with ABC. The free field analysis therefore validates only the seismic wave input method. Clearly, the proposed seismic wave input method in this paper is effect.

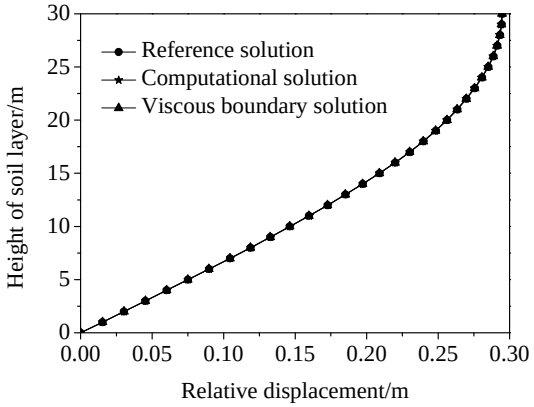

Figure 5.3. Relative displacements of artificial boundary nodes at instant of peak value displacement

A concrete structure of box shape is constructed in the soil layer. Its width is 10 m, height 8 m and thickness 1 m. The mass density and shear modulus of concrete are 2450 kg/m^3 and 1.568 GPa, respectively, leading to shear wave velocity 800 m/s. No nonlinearity is considered in near field, because the work in this paper concentrates on the ABC and wave input method. Because no analytical solution can be obtained in this case, the finite element solution in a sufficient large domain is used as an "exact" reference solution. The computational solutions of structure cannot be distinguished from the corresponding reference solutions. As the more rigorous verification, the responses on artificial boundary are given. At the instant (7.54875 s) when the relative displacement at point B reaches a peak value (0.2319 m), the relative displacements on artificial boundary nodes are shown in Fig. 5.4. Clearly, the computational solution is so accurate that it cannot be distinguished from the reference solution. The viscous boundary solutions are also given in Fig. 5.4. The max relative error of the relative displacements on artificial boundary nodes is only 1.82 % for the proposed ABC, while it is up to 23.5 % for the viscous boundary. Clearly, the proposed ABC has high accuracy, while the accuracy of viscous boundary cannot be accepted. The responses in Fig. 5.4 are smaller than the free-field responses in Fig. 5.3. The reason may be that a structure of more rigid than soil is introduced to lead to a more rigid system than free field site.

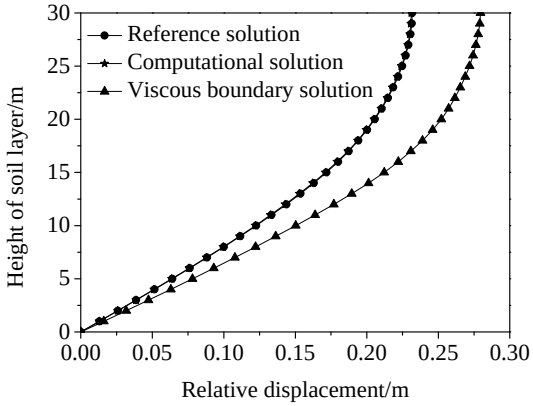

Figure 5.4. Relative displacements on artificial boundary nodes at instant of peak value displacement

6. CONCLUSIONS

A time-domain direct method is presented for the seismic soil-structure interaction analysis. It consists of finite element method, high-order accurate artificial boundary condition (ABC) and seismic wave input method. The ABC has high accuracy and is a relation of force and displacement on artificial boundary which is compatible very well with finite element method. The seismic waves are transformed into the nodal forces acting on all artificial boundary nodes. The time-domain direct method has higher accuracy than the method using viscous boundary, and it is an explicit scheme applicable to the large-scale problem and long-time computation. In this paper the out-of-plane wave motion of a homogenous soil layer resting on a rigid rock is considered. The elastic wave and multilayered soil problem will be studied in future.

AKCNOWLEDGEMENT

This work is supported by National Basic Research Program of China (2011CB013602), National Natural Science Foundation of China (51008170), Beijing Nova program (2011017), China Postdoctoral Science Foundation, and Project for Supervisor of Chinese and Beijing Excellent Doctoral Dissertation.

REFERENCES

Bazyar, M.H. and Song, C. (2008). A continued-fraction-based high-order transmitting boundary for wave propagation in unbounded domains of arbitrary geometry. *International Journal of Solids and Structures*. **74:** 209-237.

Birk, C. and Ruge, P. (2007). Representation of radiation damping in a dam-reservoir interaction analysis based on a rational stiffness approximation. *Computers and Structures*, **85:** 1152-1163.

Du, X. and Zhao, M. (2010a). Stability and identification for rational approximation of frequency response function of unbounded soil. *Earthquake Engineering and Structural Dynamics*. **39: 2**, 165-186.

Du, X. and Zhao, M. (2010b). A local time-domain transmitting boundary for simulating cylindrical elastic wave propagation in infinite media. *Soil Dynamics and Earthquake Engineering*. **30: 10**, 937-946.

Givoli, D. (1999). Recent advances in the DtN FE method. *Archives of Computational Methods in Engineering*. **6:** 71-116.

Guddati, M.N. and Tassoulas, J.L. (1999). Space-time finite elements for the analysis of transient wave propagation in unbounded layered media. *International Journal of Solids and Structures*. **36:** 4699-4723.

Joyner, W.B. and Chen, A.T.F. (1975). Calculation of nonlinear ground response in earthquake. *Bulletin of the Seismological Society of America*. **65:** 1315-1336.

Liu, J. and Lü, Y. (1997). A Direct Method for Analysis of Dynamic Soil-Structure Interaction based on Interface Idea. *Chinese-Swiss Workshop on Dynamic Soil-Structure Interaction*. 258-273.

Liu, T. and Xu, Q. (2002). Discrete artificial boundary conditions for transient scalar wave propagation in a 2D unbounded layered media. *Computer Methods in Applied Mechanics and Engineering*, **191:** 3055-3071.

Liu, T. and Zhao, C. (2010). Finite element modeling of wave propagation problems in multilayered soils resting on a rigid base. *Computers and Geotechnics*. **37:** 248-257.

Lysmer, J. and Kuhlemeyer, R.L. (1969). Finite dynamic model for infinite media. *Journal of the Engineering Mechanics Division, ASCE*. **95:** 869-877.

Lysmer, J. and Waas, G. (1972). Shear waves in plane infinite structures. *Journal of the Engineering Mechanics Division, ASCE*. **98:** 85-105.

Wang, J., Zhang, C. and Du, X. (2008). An explicit integration scheme for solving dynamic problems of solid and porous media. *Journal of Earthquake Engineering*. **12:** 293-311.

Wolf, J.P. (1988). Soil-Structure-Interaction Analysis in Time Domain. Prentice Hall, Englewood Cliffs, N.J.

Yasui, Y., Takano, S., Takeda, T., et al. (1988). Finite Element Method for Obliquely Incident Seismic Wave Problems. *Ninth World Conference on Earthquake Engineering*. **Vol III:** 447-452.

Zhao, M., Du, X. and Liu, J. (2010). Explicit Finite Element Artificial Boundary Scheme for Wave Equation on Unbounded Domain. *Eleventh International Symposium on Structural Engineering*. **Vol I:** 1164-1169.

Zhao, M., Du, X., Liu, J. and Liu, H. (2011). Explicit finite element artificial boundary scheme for transient scalar waves in two-dimensional unbounded waveguide. *International Journal for Numerical Methods in Engineering*. **87: 11**, 1074-1104.

Zienkiewicz, O.C. and Taylor, R.L. (2008). The Finite Element Method for Solid and Structural Mechanics (6th edn). Elsevier, Singapore.